

# Parallel between infrared characterisation and ab initio calculations of CO adsorption on sulphided Mo catalysts

A. Travert<sup>a</sup>, C. Dujardin<sup>a</sup>, F. Maugé<sup>a,\*</sup>, S. Cristol<sup>b</sup>,  
J.F. Paul<sup>b</sup>, E. Payen<sup>b,1</sup>, D. Bougeard<sup>c</sup>

<sup>a</sup> UMR CNRS 6506, Laboratoire de Catalyse et Spectrochimie, ISMRA-6, boulevard du Maréchal Juin, 14050 Caen Cedex, France

<sup>b</sup> UPRESA CNRS 8010, Laboratoire de Catalyse, bât. C3, Université des Sciences et Technologies de Lille,  
59650 Villeneuve d'ascq Cedex, France

<sup>c</sup> UMR CNRS 8516, bât. C5, Université des Sciences et Technologies de Lille, 59650 Villeneuve d'ascq Cedex, France

## Abstract

Carbon monoxide adsorption on sulphided Mo catalysts has been investigated by means of IR spectroscopy and DFT ab initio calculations. IR experiments show that CO adsorption on the sulphide phase of Mo/Al<sub>2</sub>O<sub>3</sub> catalysts gives rise to various  $\nu(\text{CO})$  bands, the intensities of which are strongly modified when post-treatment of the catalyst with H<sub>2</sub> or H<sub>2</sub>S is performed before CO adsorption, therefore, revealing strong modifications in the nature and the number of sites present on the sulphide phase. Ab initio periodic DFT calculations allow to define two types of edges for MoS<sub>2</sub>, which sulphur coverage and structure depend on the H<sub>2</sub>/H<sub>2</sub>S ratio in the surrounding atmosphere. Adsorption energies and stretching wavenumber of CO adsorbed on the various sites of these surfaces were computed, providing the possibility to compare for the first time results from theoretical calculations and spectroscopic measurements on these systems. A novel attribution of the main IR features of CO adsorbed on MoS<sub>2</sub> is proposed. © 2001 Elsevier Science B.V. All rights reserved.

**Keywords:** Infrared spectroscopy; Density functional theory; Carbon monoxide; Hydrotreating catalysts

## 1. Introduction

Improvement in the hydrodesulphurisation (HDS) of the petroleum feedstocks has been driven by the need to produce clean fuels based on the pressing requirement for environmental protection. HDS is generally performed with Mo-based catalysts, the active phase of which consists of molybdenum disulphide nanocrystallites well dispersed on an alumina support. Molybdenum disulphide is a highly anisotropic material and it is now well admitted that the Mo coordinative unsaturated sites (CUSs) located at the edges

of these nanocrystallites play a major role in the adsorption and the activation of the reactants. Although a considerable amount of research has been made on these systems, an accurate description of these sites is still lacking. A convenient way to characterise such sites is the use of probe molecule adsorption. In this way, oxygen and nitrogen monoxide were found particularly well suited, because they specifically adsorb on the sulphide phase. NO presents the additional advantage to be easily detected by IR spectroscopy, providing informations on the nature and the amount of the different sites on which it is anchored. However, it has been recognised on time that NO as well as O<sub>2</sub> lead to a partial oxidation of the sulphide, even at very low temperatures [1]. The reliability of these

\* Corresponding author.

<sup>1</sup> Co-corresponding author.

methods may therefore be questioned: experimental parameters as the adsorption temperature or the contact time of the probe with the surface are expected to strongly influence the oxidation state of the sulphide phase and accordingly the interaction of the probe with the surface. Indeed, many disagreements are found in the literature on the IR observations of NO adsorbed on sulphided Mo catalysts [2].

On the other hand, carbon monoxide that is otherwise widely used for the IR characterisation of metal oxides and supported metals, has been more scarcely employed in the case of sulphided catalysts. Its worth, however, has been demonstrated by several studies among which Lavalley's group brought major contributions. Indeed, recognising the oxidant behaviour of probes such as O<sub>2</sub>, Bachelier et al. [3] firstly proposed the use of carbon monoxide as an alternative probe. The totally reversible adsorption of CO on the sulphide phase was demonstrated and some correlations were obtained between the CO uptake and HDS activities of Mo-based catalysts [3]. The first IR observations of CO adsorption on sulphided Mo catalysts were reported by Peri [4], showing a broad band at ca. 2100 cm<sup>-1</sup> characteristic of CO adsorbed on the sulphide phase. Apart from this main feature, Bachelier et al. [5] could also evidence the presence of a weak component at ca. 2070 cm<sup>-1</sup>, further reported by Müller et al. [6]. Last, by means of CO–NO co-adsorption experiments, Qin et al. [7] were able to distinguish another component in the broad band at ca. 2090 cm<sup>-1</sup>. In spite of the complexity of the spectrum in that spectral range, Maugé and Lavalley [8] determined its mean extinction coefficient, allowing therefore quantitative evaluation of the amount of sites on sulphided Mo/Al<sub>2</sub>O<sub>3</sub> catalyst, which they correlated with their activities. A quantitative relationship was further obtained with the number of Mo atoms located at the edge of the sulphide crystallites as determined by HREM measurements [9,10].

Therefore, the sites probed by CO are likely to play an important role in hydrotreating catalysis. In this respect, IR spectroscopy of adsorbed CO could significantly improve our knowledge of the active surface of sulphided Mo catalysts. However, the interpretation of the IR spectra is not straightforward and, on the basis of qualitative arguments, most of workers were in trouble to give a precise attribution of the observed  $\nu(\text{CO})$  bands. Accordingly, Peri [4]

defined the CUS sites responsible for CO adsorption as Mo<sup>δ+</sup> sites resulting from the interaction of Mo<sup>0</sup> with Mo<sup>4+</sup> centres, this interpretation being later adopted by Zaki et al. [11]. On the other hand, Bachelier et al. [5] proposed that the main feature at 2100 cm<sup>-1</sup> correspond to the adsorption on reduced Mo<sup>x+</sup> centres, whereas the component at 2070 cm<sup>-1</sup> would be due to the adsorption on more reduced Mo atoms. In the same time, Delgado et al. [12] proposed for these species a formal oxidation state of +2, which would result from the reduction of surface Mo during the sulpho-reduction. Last, Müller et al. [6] attributed the component at 2070 cm<sup>-1</sup> to Mo atoms located on the corner of the sulphide crystallites.

Finally, the nature and the location of the sites on which CO adsorb is still under debate and IR spectroscopy — as a single technique — is unlikely to provide an answer. Modelling of these nanocrystallites is one possible approach to get a better insight into the nature of the sites. The recent development of new molecular modelling techniques, especially DFT, now allows one to define more and more realistic sulphide surfaces. Raybaud et al. [13] published an ab initio investigation of the structural and electronic properties of the clean MoS<sub>2</sub> (0 1 0) edge surface using the Vienna ab initio simulation program (VASP). These authors showed that the as-cleaved (1 0 0) edge surface remains stable in vacuum up to temperatures of  $T = 700 \text{ K}$  [14]. The sulphur coverage of the MoS<sub>2</sub> edge surfaces, which depends on the operating conditions through the relative chemical potential of H<sub>2</sub> and H<sub>2</sub>S in the surrounding atmosphere, was later developed [15,16]. These works allowed the calculation of different edge surfaces, the domains of existence of which are defined by the H<sub>2</sub> pressure and the H<sub>2</sub>/H<sub>2</sub>S ratio.

The aim of the present work is to use molecular modelling techniques to assign the stretching frequencies of CO adsorbed on an unpromoted MoS<sub>2</sub> catalyst. We will first present FTIR experiments in which the distribution of the Mo sites is varied by the pre-treatments of the sulphided sample. Then the MoS<sub>2</sub> (1 0 0) stable surfaces and the stretching frequencies of CO adsorbed on these surfaces deduced from the calculations will be presented. We will finally compare both the methods of investigation and discuss the attribution of the IR bands in relation with our model.

## 2. Experimental

### 2.1. IR spectroscopy

#### 2.1.1. Catalysts

Two Mo/Al<sub>2</sub>O<sub>3</sub> samples, 8Mo and 9Mo, containing, respectively, 8 and 9 wt.% molybdenum were prepared by impregnation of the alumina support ( $S_{\text{BET}} = 220 \text{ m}^2 \text{ g}^{-1}$ ) with an ammonium heptamolybdate solution, followed by drying and calcination at 773 K. Before introduction in the IR cell, the oxide precursors so obtained were grounded, pressed into self-supported wafers (ca.  $5 \text{ mg cm}^{-2}$ ).

#### 2.1.2. Sulphidation

The sulphidation was carried out in situ in the IR cell according to the following procedure. After outgassing at 523 K, the catalysts were contacted with 100 Torr (1 Torr =  $133.3 \text{ N m}^{-2}$ ) of a H<sub>2</sub>S/H<sub>2</sub> (15/85) mixture and heated at a rate of  $10 \text{ K min}^{-1}$  up to 673 K and further maintained at this temperature. The sulphidation was followed by an evacuation of 10 min at the same temperature. The sulphidation–evacuation cycle was repeated three times, the duration of sulphidation being, respectively, 1.5, 12 and 1.5 h. The last evacuation was performed up to a residual pressure of  $2 \times 10^{-6}$  Torr. The catalysts treated in such a way will be named “sulphided catalysts” in the following parts and will be denoted as 8Mo(S) and 9Mo(S).

A set of experiments was also performed on the 9Mo sample after an ex situ pre-sulphidation. In this case, the oxide precursor was sulphided under a flow of H<sub>2</sub>S/H<sub>2</sub> (15/85) mixture at 623 K, further ground and pressed into a self-supported pellet in the laboratory atmosphere before introduction in the IR cell. This catalyst will be denoted as 9Mo(exS).

#### 2.1.3. Post-treatments

The sulphided 8Mo(S) and 9Mo(S) catalysts were subjected to various post-treatments before or between CO adsorption experiments.

1. *Hydrogen treatments.* The 8Mo(S) catalyst was evacuated at 673 K and further cooled down to the reduction temperature (473, 573 and 673 K). Then, the catalyst was contacted with 250 Torr H<sub>2</sub> during 30 min at the chosen temperature followed by an evacuation of 10 min at the same temperature.

Two reduction–evacuation cycles were done in order to remove the H<sub>2</sub>S formed upon reduction. The last evacuation was performed up to a residual pressure of  $6 \times 10^{-6}$  Torr. The solids will be denoted as Mo(SR-T), where T is the temperature of reduction.

2. *H<sub>2</sub>S treatments.* Another set of experiments was performed on 9Mo(S) and consisted in the following sequence. After in situ sulphidation of the catalyst, successive calibrated doses of H<sub>2</sub>S were introduced at room temperature (RT). After each H<sub>2</sub>S dose, the catalyst was cooled down to 100 K and characterised by CO adsorption. Before introducing the following H<sub>2</sub>S dose at RT, the cell was maintained under dynamic vacuum from 100 up to 673 K in order to completely desorb CO. Then, the catalyst was re-sulphided at 673 K for 30 min, degassed up to a residual pressure of  $5 \times 10^{-6}$  Torr was reached and further cooled down at RT, allowing the introduction of another dose of H<sub>2</sub>S in the cell. We have checked that these successive treatments did not modify the catalyst surface state before the introduction of a given dose of H<sub>2</sub>S.

#### 2.1.4. CO adsorption

The adsorption of CO has then been characterised by FTIR. Before IR characterisation, the catalysts were contacted with 0.5 Torr of He at RT, for a better thermal contact at low temperature, and further cooled down to 100 K. Small calibrated doses of CO were introduced in the IR cell up to an equilibrium pressure of 1 Torr. CO was further evacuated at low temperature ( $P = 1 \times 10^{-4}$  Torr). FTIR spectra were recorded in 256 scans after each CO introduction using a 60SX Nicolet FTIR spectrometer with a resolution of  $4 \text{ cm}^{-1}$ .

In all these experiments, CO as well as H<sub>2</sub> and He were purified by trapping in liquid nitrogen before contact with the catalyst. H<sub>2</sub>S was purified by distillation at low temperature (77–160 K).

## 2.2. Computational techniques

The periodic DFT calculations were performed with the VASP [17–20], based on plane waves that allows a good description of the MoS<sub>2</sub> surface, by using large supercells ( $9.48 \times 12.294 \times 20 \text{ \AA}^3$ ). Fig. 1 shows the cell that has been used for the calculations. As shown in a previous study [14,15], such a model containing

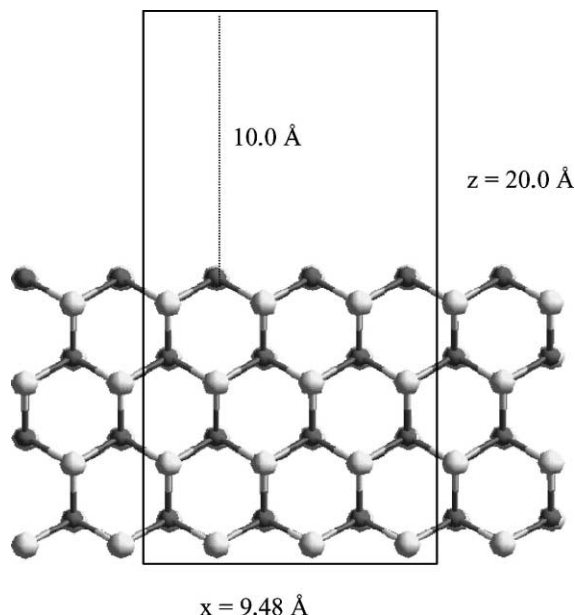


Fig. 1. Representation of the supercell used for calculations, showing the axes. Dark circles: Mo; light circles: S.

two layers along the  $y$ -direction, three rows in the  $x$ -direction and four in the  $z$ -direction is suitable to give a good description of the structural and adsorption properties of the (100) MoS<sub>2</sub> surface. All over this work, we used a cut-off energy of  $E_{\text{cut}} = 300$  eV,

a Methfessel–Paxton [21] smearing with  $\sigma = 0.1$  eV and  $\Gamma$  point for Brillouin zone integration. The two upper rows and the adsorbed molecules were allowed to relax during the calculation, while the two lower ones were kept fixed at the bulk geometry. In order to compute reliable adsorption energies, the non-local functional using generalised gradient corrections (GGA) of Perdew et al. [22,23] was applied. The CO vibration frequencies were calculated by numerical differentiation of the force matrix. In order to reduce the computation time, we computed only the part of the matrix corresponding to the three or six atoms closest to CO. As isotopic substitution suggests that the CO stretching vibration mode is only very weakly coupled with the vibrations of the surface, this approximation should not induce important systematic errors. All the calculated frequencies are scaled by 1.02, a factor used to fit calculated and experimental CO stretching vibration of the free CO molecule.

### 3. Results

#### 3.1. IR characterisation of CO adsorption

##### 3.1.1. Sulphided catalyst

The IR spectra of CO adsorbed on sulphided 8Mo catalyst are presented in Fig. 2. Three main bands at

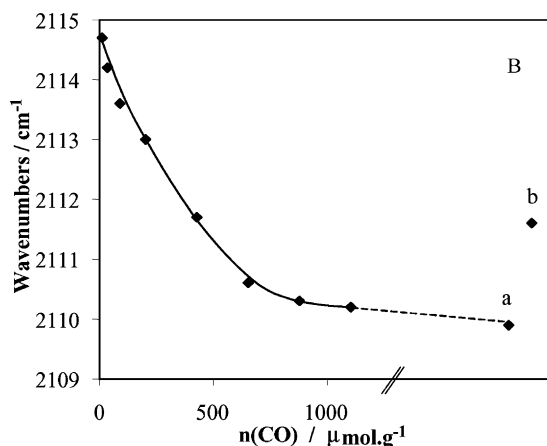
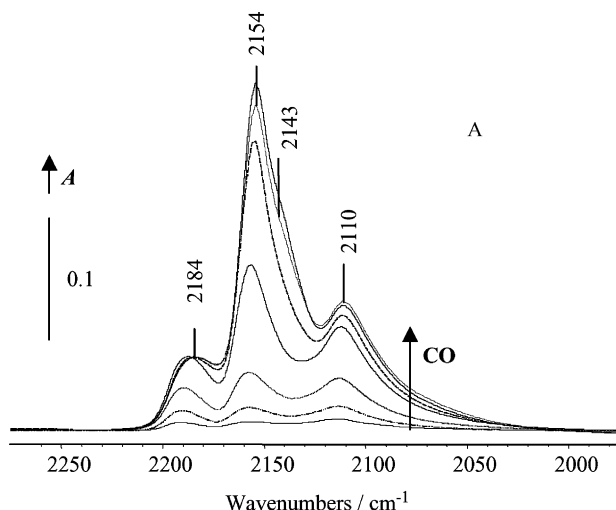


Fig. 2. (A) IR spectra of increasing doses of CO adsorbed at 100 K on sulphided 8Mo(S) catalyst. (B) Variation of the wavenumber of CO/Mo band versus the CO doses (a: 1 Torr of CO at equilibrium; b: CO evacuated up to  $P = 2 \times 10^{-5}$  Torr).

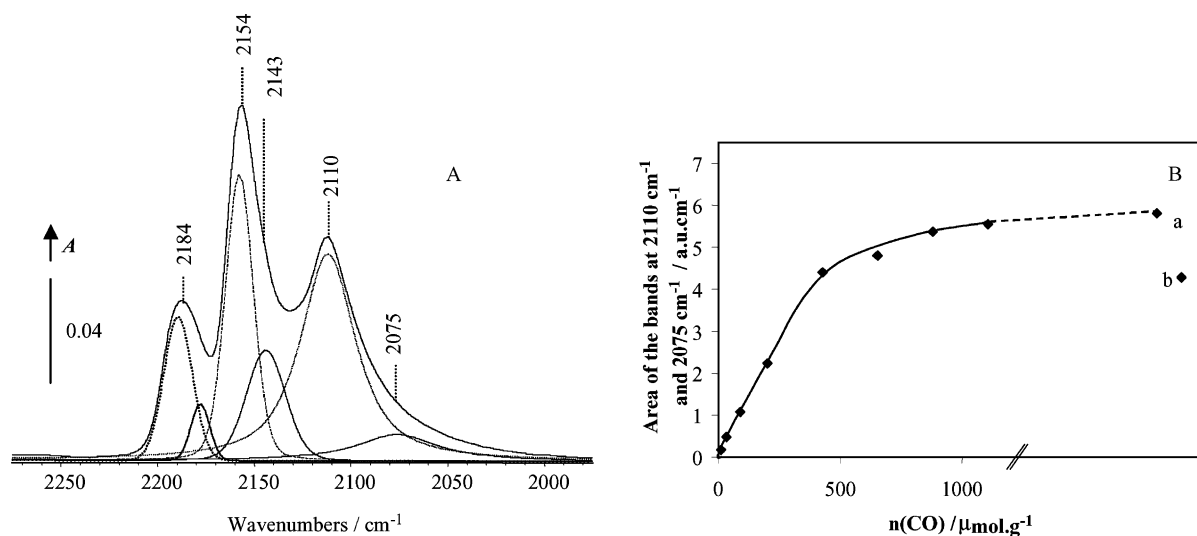


Fig. 3. (A) Decomposition of the IR spectra for  $429 \mu\text{mol g}^{-1}$  of CO adsorbed at 100 K on sulphided 8Mo(S) catalyst. (B) Variation of the area of CO/Mo bands at 2110 and  $2075 \text{ cm}^{-1}$  versus CO doses (a: 1 Torr of CO at equilibrium; b: CO evacuated up to  $P = 2 \times 10^{-5}$  Torr).

$2184$ ,  $2154$  and  $2110 \text{ cm}^{-1}$  are observed, the intensity of which increases with the amount of CO introduced. From previous studies [6,8], these bands can be attributed, respectively, to coordination of CO on Lewis acid sites of the alumina support, CO in hydrogen bonding with the support hydroxyl groups and to CO in interaction with the edges of the  $\text{MoS}_2$  nanocrystallites. At high CO uptake, a shoulder at  $2143 \text{ cm}^{-1}$ , corresponding to physisorbed CO, appears. Upon degassing at 100 K, a strong decrease of the intensity of the band characterising physisorbed CO and CO interacting with the support is noticed. By evacuation at 295 K, all the CO bands are eliminated except a small shoulder at ca.  $2075 \text{ cm}^{-1}$  [5].

A careful analysis of the spectra shows that the band characteristic of CO adsorbed on the disulphide crystallites shifts with the increase of the CO uptake. Introduction of the first dose of CO leads to the appearance of a main band at  $2115 \text{ cm}^{-1}$  with a shoulder at  $2126 \text{ cm}^{-1}$ . The wavenumber at the maximum of the predominant band shifts from  $2115$  to  $2110 \text{ cm}^{-1}$  for 1 Torr CO at equilibrium and slightly increases up to  $2112 \text{ cm}^{-1}$  after evacuation (Fig. 2B). In order to obtain more accurate information about the sites characterised by this band, decomposition of the spectra obtained after introduction of various CO doses was performed. The decomposition of the

spectrum corresponding to an intermediate CO dose is reported in Fig. 3A. The asymmetry of the band at  $2110 \text{ cm}^{-1}$  required generating a weak band at ca.  $2075 \text{ cm}^{-1}$  to correctly fit the experimental spectrum. The presence of such a low wavenumber  $\nu(\text{CO})$  band has already been reported by Bachelier et al. [5] and more recently by Müller et al. [6]. Its absorbance is weak, indicating that the corresponding number of adsorbed CO molecules should be low as the molar extinction coefficient usually increases as the  $\nu(\text{CO})$  wavenumber decreases. Thus after sulphidation, the 8Mo(S) catalyst presents mainly Mo sites corresponding to the  $2110 \text{ cm}^{-1}$  band.

Decomposition of the spectra recorded at various CO coverages shows that the area of bands characterising Mo sites are maximum from ca.  $500 \mu\text{mol g}^{-1}$  (Fig. 3B), a value that correspond to the saturation of the sites. After introduction of 1 Torr CO at equilibrium, the area of these bands remains very close to the values measured at saturation.

### 3.1.2. Effect of $\text{H}_2\text{S}$ adsorption on sulphided catalyst

The effect of the introduction of increasing doses of  $\text{H}_2\text{S}$  at RT on the CO adsorption spectra of 9Mo(S) catalyst is presented in Fig. 4A and B.

$\text{H}_2\text{S}$  pre-adsorption leads to a decrease of the intensity of the bands characterising CO coordinated

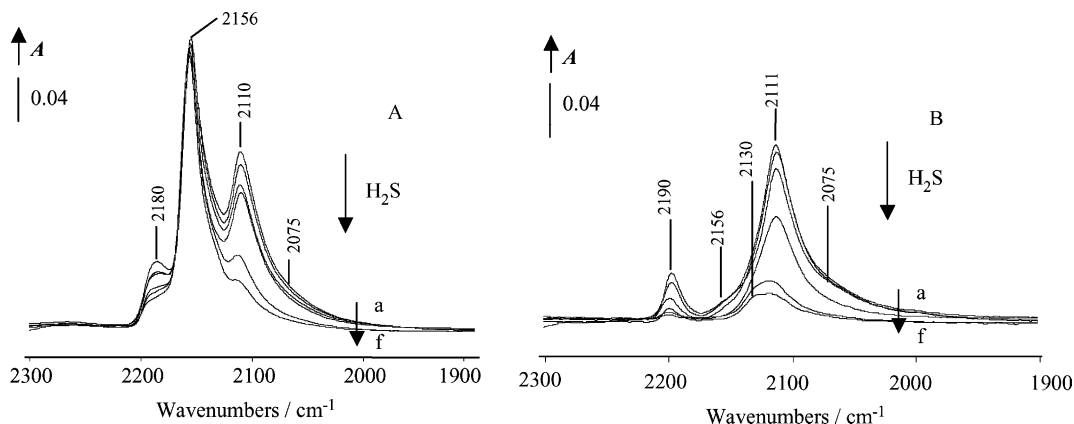


Fig. 4. IR spectra of CO adsorbed at 100 K after introduction of increasing doses of  $\text{H}_2\text{S}$  at RT (a, b, c, d, e = 0, 40, 50, 96,  $240 \mu\text{mol g}^{-1}$ , respectively; f = 5 Torr at equilibrium) on sulphided 9Mo(S) catalyst: (A) 1 Torr of CO at equilibrium; (B) CO evacuated up to  $P = 2 \times 10^{-5}$  Torr.

on the support and to a slight increase of the high frequency side of the band at  $2155 \text{ cm}^{-1}$  (H-bonded CO). A careful analysis of alumina hydroxyl bands (not presented here) shows the creation of some new acidic OH groups due to  $\text{H}_2\text{S}$  dissociative adsorption. As for CO in interaction with the  $\text{MoS}_2$  slabs, an important decrease in the intensity of the band at  $2110 \text{ cm}^{-1}$  as well as of the shoulder at  $2075 \text{ cm}^{-1}$  is observed. No preferential variation of these bands with the adsorption of  $\text{H}_2\text{S}$  could be noticed. At high  $\text{H}_2\text{S}$  coverage, the intensity of the  $2110 \text{ cm}^{-1}$  band is very weak and after CO evacuation at ca. 100 K, a shoulder is observed at  $2130 \text{ cm}^{-1}$  (Fig. 4B). One cannot consider that this band originates from  $\text{H}_2\text{S}$  introduction as it could be present before its introduction and be hidden by the intense band at  $2110 \text{ cm}^{-1}$ . Moreover, it should be noted that a small band at such a high wavenumber can also be noticed when a few amount of CO is adsorbed on the 8Mo(S) catalyst.

Finally, the global decrease in the intensity of the  $\nu(\text{CO}/\text{MoS}_2)$  massif after  $\text{H}_2\text{S}$  pre-adsorption indicates a partial poisoning of the sites of  $\text{MoS}_2$  edges by sulphur species.

### 3.1.3. Effect of an ex situ pre-sulphidation

CO adsorption has been performed after in situ re-sulphidation of an ex situ pre-sulphided catalyst. Surprisingly, CO adsorption on the 9Mo(exS) reveals a very low number of Mo sites (Fig. 5), whereas the various adsorption mode on the support are not mod-

ified by the sample preparation. The comparison of the spectra of CO adsorbed on 9Mo(S) and 9Mo(exS) catalysts points out that the Mo sites giving rise to the band at  $2110 \text{ cm}^{-1}$  are preferentially poisoned, while those corresponding to the  $\nu(\text{CO})$  shoulder at ca.  $2065 \text{ cm}^{-1}$  do not seem to be affected by this treatment. This shows that once they are poisoned by such a treatment, the Mo sites giving rise to the band at  $2110 \text{ cm}^{-1}$  cannot be restored by a re-sulphidation. Such deep modifications of the catalyst by air contact have already been reported [24].

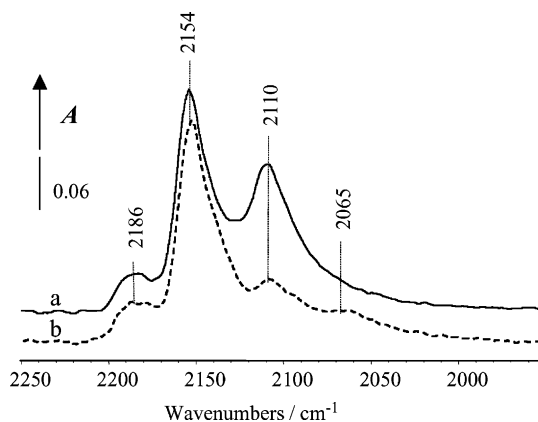


Fig. 5. Comparison of the IR spectra of 1 Torr CO at equilibrium at 100 K adsorbed on 9Mo catalyst either directly sulphided in the IR cell (a) or pre-sulphided ex situ and re-sulphided in the IR cell (b).

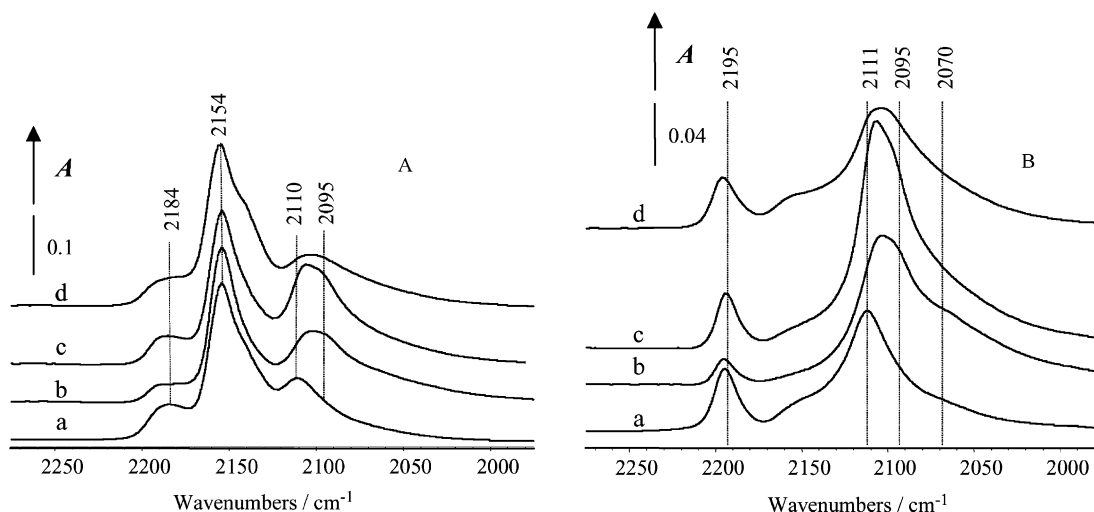


Fig. 6. IR spectra of CO adsorbed at 100 K after various treatment of 8Mo catalyst. (A) 1 Torr of CO at equilibrium; (B) CO evacuated up to  $P = 2 \times 10^{-5}$  Torr (a: sulphided catalyst; b: a +  $H_2$  treatment at 473 K; c: b +  $H_2$  treatment at 573 K; d: b +  $H_2$  treatment at 673 K).

Such a selective poisoning clearly confirms the presence of two kinds of edge sites on the  $MoS_2$  slabs giving rise to  $\nu(CO)$  bands at  $2110\text{ cm}^{-1}$  (strong) and at a wavenumber lower than  $2080\text{ cm}^{-1}$  (weak).

#### 3.1.4. Effect of a hydrogen treatment

The  $\nu(CO)$  spectra obtained after a hydrogen treatment of the 8Mo(S) catalyst are presented in Fig. 6A and B. A strong increase in the intensity of the bands characterising CO adsorption on the sulphide phase is observed up to a reduction temperature of 573 K. Indeed, the corresponding band area is more than twice higher after post-reduction at 573 K than after sulphidation. By contrast, as already reported by Müller et al. [6], intensity of these  $\nu(CO)$  bands is strongly decreased after reduction of the catalyst at 673 K.

Besides these variations of intensities, changes in the shape of the  $\nu(CO/MoS_2)$  massif are also observed. To analyse precisely these modifications induced by reduction, spectra corresponding to introduction of the various CO doses on 8Mo(S) and 8Mo(SR-473) are compared in Fig. 7A. They provide evidence for a decrease in the number of Lewis acid sites of the support upon reduction ( $\nu(CO) = 2191\text{ cm}^{-1}$ ) as well as an increase in the number of OH groups ( $\nu(CO) = 2156\text{ cm}^{-1}$ ). The band characteristic of the adsorption on the  $MoS_2$  crystallites is also affected. In particular, the maximum of the massif initially present

at  $2110\text{ cm}^{-1}$  on the sulphided sample is shifted to  $2105\text{ cm}^{-1}$ , whereas a shoulder at ca.  $2095\text{ cm}^{-1}$  and a broad feature centred at ca.  $2055\text{ cm}^{-1}$  develop after reduction. One should note that the shift of the maximum of the massif towards lower wavenumbers after reduction cannot be related to a modification of the CO coverage, since it is observed even for the first CO doses. Thus, the increase of the  $\nu(CO/MoS_2)$  massif area as well as the occurrence of new bands shows the creation of new Mo sites upon reduction.

To compare the effect of reduction temperature, the difference between spectra (1 Torr of CO at equilibrium) obtained after successive treatments have been computed and are presented in Fig. 7B. Spectrum 7B-a shows that reduction at 473 K leads to appearance of a band at ca.  $2095\text{ cm}^{-1}$  with a shoulder at  $2105\text{ cm}^{-1}$ , and a broad, low wavenumber feature presenting a maximum at ca.  $2055\text{ cm}^{-1}$  with a tail extending down to  $2020\text{--}2000\text{ cm}^{-1}$ . Spectrum 7B-b shows that reduction at 573 K — compared to reduction at 473 K — induces an increase in the number of sites characterised by the bands at 2095 and  $2105\text{ cm}^{-1}$ . A slight increase in intensity is also observed at ca.  $2075\text{ cm}^{-1}$ , whereas in contrast with the previous spectrum, no significant variation of absorbance at lower wavenumbers is observed between reduction at 473 and 573 K. The negative intensity of the spectra difference presented Fig. 7B-c indicates that reduction at 673 K

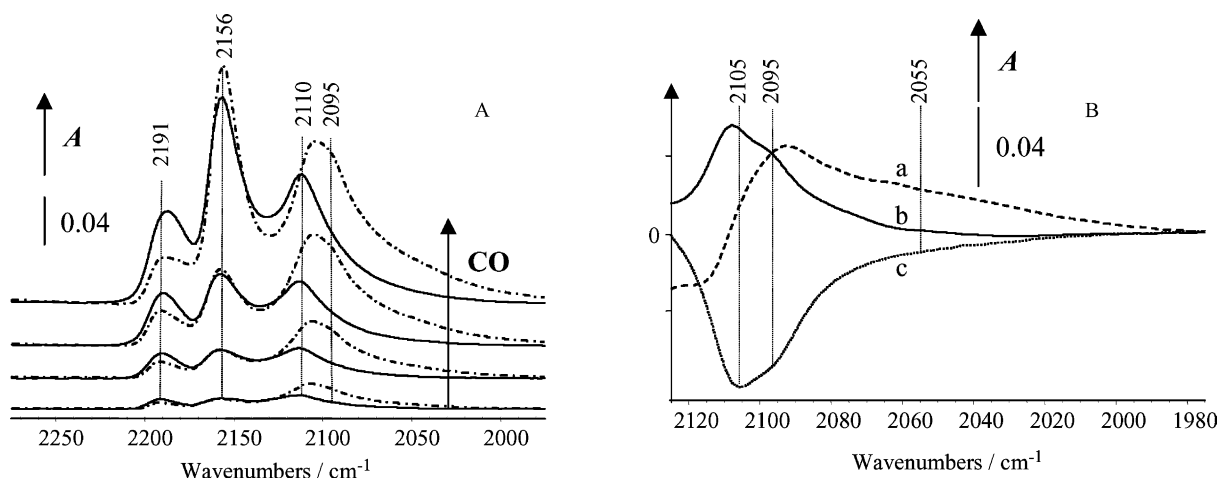


Fig. 7. (A) Comparison of IR spectra of increasing small calibrated CO doses adsorbed at 100 K on 8Mo catalyst either sulphided (—) or sulphided and reduced at 473 K (-----). (B) Difference between spectra corresponding to adsorption of 1 Torr CO at equilibrium at 100 K for two successive treatments of 8Mo catalyst (a: reduced at 473 K minus sulphided; b: reduced at 573 K minus reduced at 473 K; c: reduced at 673 K minus reduced at 573 K).

induces a decrease in the number of sites characterised by bands at 2105 and at 2095  $\text{cm}^{-1}$ , the disappearance of the band at 2105  $\text{cm}^{-1}$  being more marked.

Decomposition of the spectra of the reduced catalysts was also performed. It appeared that the  $\nu(\text{CO}/\text{MoS}_2)$  massif could not be correctly fitted with only the two bands at ca. 2110 and ca. 2055  $\text{cm}^{-1}$  which were adequate in the case of the sulphided catalyst. In particular, a third band at ca. 2095  $\text{cm}^{-1}$  had to be introduced, confirming the creation of new sites upon reduction. However, although some trends in the variation of the number of sites appear, no quantitative analysis of these modifications can be performed at present, since the molar extinction coefficient of the individual  $\nu(\text{CO})$  bands is not known.

Finally, from the analysis of the spectral range characteristic of the adsorption on the  $\text{MoS}_2$  edges, several  $\nu(\text{CO})$  components can be distinguished as follows:

1. An intense band at ca. 2110  $\text{cm}^{-1}$  present on sulphided catalyst, which increases in intensity and undergoes a slight downward shift upon reduction.
2. A band at ca. 2130  $\text{cm}^{-1}$  which can only be noticed when very small amount of CO are present on Mo edge sites or when large amounts of  $\text{H}_2\text{S}$  are pre-adsorbed.
3. A band at ca. 2095  $\text{cm}^{-1}$  which develops only after reduction of the catalyst.

4. A broad, low wavenumber feature below 2080  $\text{cm}^{-1}$  that is partly present on freshly sulphided catalysts, increases in intensity upon reduction (below 673 K) and spreads at wavenumbers as low as 2000–2020  $\text{cm}^{-1}$ . This feature seemingly includes several components that, however, cannot be resolved due to their broadness.

### 3.2. DFT calculation

#### 3.2.1. Sulphur coverage of the $\text{MoS}_2$ crystallites

Fig. 8A is a representation of the perfect (100) crystal showing alternative rows of molybdenum and sulphur atoms. Therefore, surface of a perfect  $\text{MoS}_2$  crystal presents rows of sulphur atoms (called sulphur edge, S edge) or of molybdenum atoms (called molybdenum edge, Mo edge). This perfect surface will be denoted [6–0] as there are six sulphur atoms on the sulphur edge and no sulphur atom on the molybdenum edge. However, the exact nature of the surface stable under the HDS conditions will be defined by the chemical potential of the different species present in the gas surrounding atmosphere. Indeed in previous studies [15,16], it has been shown that the number of sulphur atoms present on the edges of the crystallites is dependent on the  $\text{H}_2/\text{H}_2\text{S}$  molar ratio and only three surfaces are thermodynamically stable



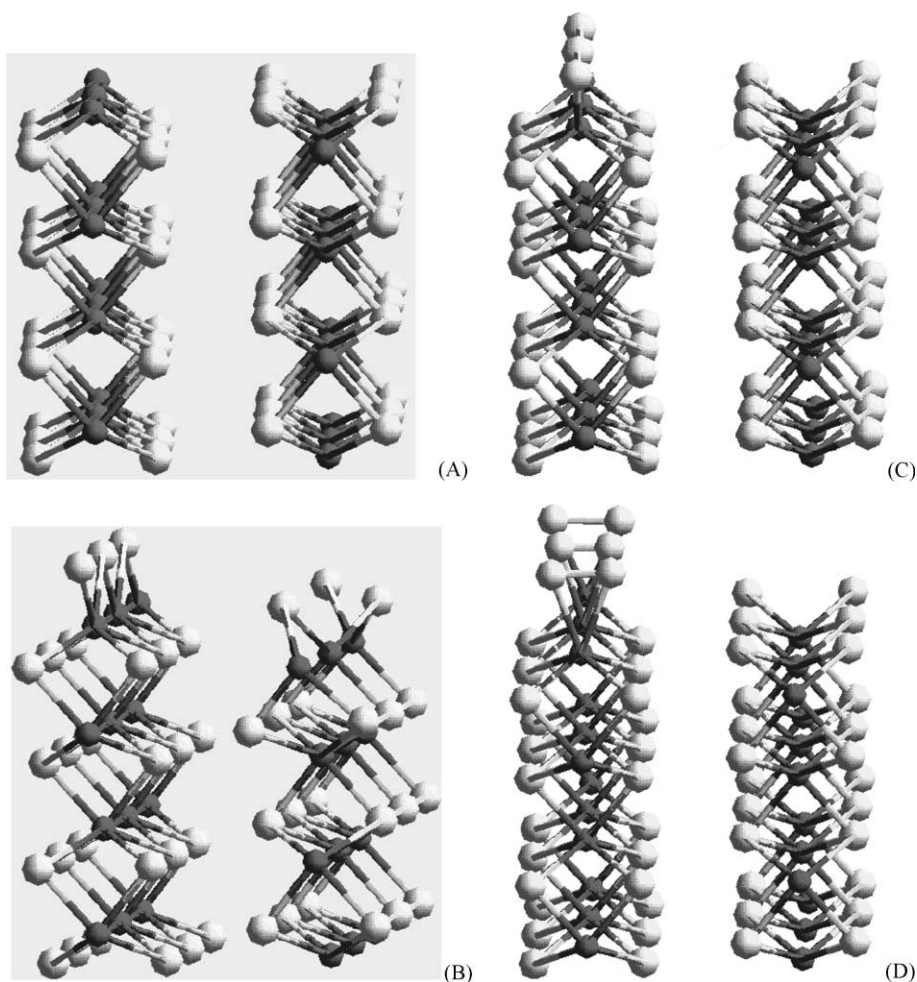


Fig. 8. Representation of the surface modification with the  $\text{H}_2/\text{H}_2\text{S}$  partial pressure: (A) perfect (1 0 0)  $\text{MoS}_2$  surface [6–0]; (B) surface [3–3], stable surface when  $\text{H}_2/\text{H}_2\text{S} > 20$ ; (C) surface [6–3], stable surface when  $10^{-4} < \text{H}_2/\text{H}_2\text{S} < 20$ ; (D) surface [6–6], stable surface when  $\text{H}_2/\text{H}_2\text{S} < 10^{-4}$ .

within the  $\text{H}_2/\text{H}_2\text{S}$  partial pressure ratio defining the zone of stability of  $\text{MoS}_2$ . These various surfaces, named as above according to the number of sulphur atoms present on each edge are shown in Fig. 8B–D according to their  $\text{H}_2/\text{H}_2\text{S}$  domain of stability.

In reductive conditions (hydrogen rich atmosphere:  $\text{H}_2/\text{H}_2\text{S} > 20$ ) the stable surface is the [3–3] one (Fig. 8B). The coordinations of the molybdenum atoms on the sulphur edge and on the molybdenum edge are, respectively, 4 ( $\text{Mo}_{4c}$ ) and 6 ( $\text{Mo}_{6c}$ ). The terminal sulphur atoms are in bridging position between two molybdenum atoms on both edges but the Mo–S

distances are similar to the distance in the crystal (2.40 Å). Considering only the coordination numbers, we can suppose that CO adsorption on the sulphur edge will be favoured in a  $\text{H}_2$ -rich environment.

Decreasing the partial pressure ratio under 20 induces a modification of the surface, the stable one being now the [6–3] one (Fig. 8C). The coordination of the molybdenum atoms of the sulphur edge is increased from 4 to 6, while the geometry of the molybdenum edge does not change. In these conditions, the geometry of the sulphur edge is similar to the geometry of the perfect (1 0 0) surface with four bridging sulphur

atoms in a plane above the surface molybdenum atoms. The coordination of Mo on both edges is now 6 which means that there is no more unsaturated site (CUS) on the edges of the crystallite. However, CO adsorption could still be possible on both edges but this adsorption will produce 7-fold coordinated molybdenum atoms.

A second transformation occurs upon decreasing the  $H_2/H_2S$  ratio ( $H_2/H_2S < 1/10^{-4}$ ) and in these  $H_2S$ -rich conditions, the stable surface is the [6–6] one (Fig. 8D). The geometry of the sulphur edge does not change, whereas the number of sulphur atoms on the molybdenum edge is increased even if the coordination number of the molybdenum does not change ( $Mo_{6c}$ ). The bridging sulphur atoms shift to a  $\mu 1$  position. So the terminal sulphur are now bounded to only one molybdenum atom.

### 3.2.2. CO adsorption

The post-treatments of the catalysts before CO adsorption were chosen to correspond to the three zones of stability of the  $MoS_2$  edge surfaces. The catalyst should thus expose three different edge surfaces. The adsorption energies of CO on each of these surfaces have been computed and are reported in Table 1.

In the intermediate range of partial pressure ratio, which approximately corresponds to the sulphiding conditions, we have to consider that the crystallites exhibit the [6–3] surface configuration that does not present any CUS site. A top adsorption on the molybdenum edge is possible, but the energy is very weak ( $E_{ads} = 0.1$  eV). Fig. 9A is a representation of the optimised structure in which CO interacts with a single Mo atom. In Fig. 9B are represented the iso-surfaces of the electronic density variation induced by the

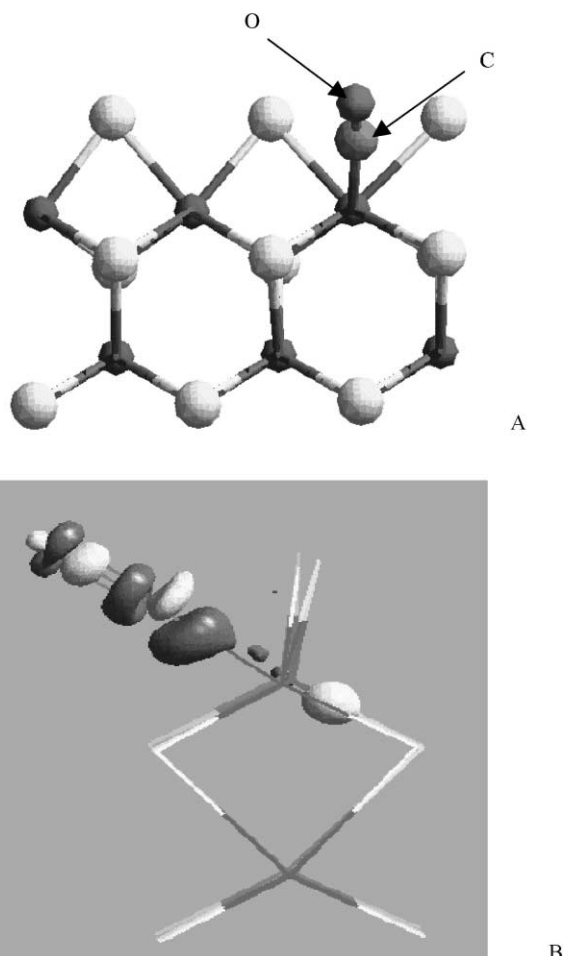


Fig. 9. Optimised configuration for one CO molecule adsorbed on the molybdenum edge [X–3]: (A) adsorption geometry; (B) electron density variation induced by the CO adsorption.

Table 1  
Comparison of the calculated properties of CO adsorbed on the various stable  $MoS_2$  edges<sup>a</sup>

Edge	Surface	Mo coordinence	$E_{ads}$ (eV)	$\nu(CO)$ ( $cm^{-1}$ )	$\Delta\nu$ ( $cm^{-1}$ ) <sup>b</sup>	$D_{Mo-C}$ (Å)	$D_{C-O}$ (Å)
Molybdenum	[X–3]	6	0.1	2080	60	1.15	2.08
	[X–6]	6	NA <sup>c</sup>	–	–	–	–
Sulphur	[6–X]	6	0.1	2040	100	1.16	2.06
	[3–X]: 1 CO/cell	4	0.7	2000	140	1.16	2.05
	[3–X]: 2 CO/cell	4	0.7	1995/2035	115	1.16	2.05
	[3–X]: 2 CO/Mo/cell	4	0.7	1965/2015	125	1.16	2.05

<sup>a</sup> The calculated free CO stretching vibration is  $2143\text{ cm}^{-1}$ .

<sup>b</sup> Difference between the calculated stretching wavenumber of the free CO molecule and the adsorbed one.

<sup>c</sup> No adsorption.

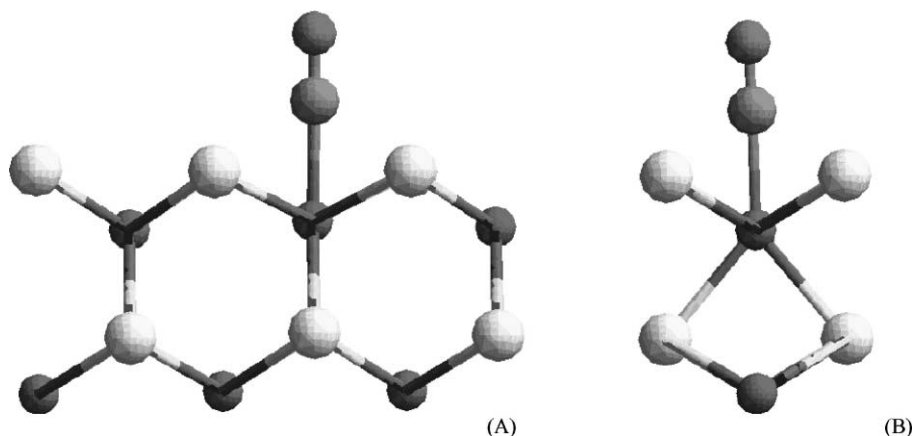


Fig. 10. Optimised configuration for one CO molecule adsorbed on the sulphided sulphur edge [6-X]: (A) front view; (B) side view.

adsorption. The important increase in this density (dark region) between the carbon and the molybdenum reflects the formation of the Mo–C bond. This is the result of electron transfer from both the non-bonding  $\sigma$  CO orbital and the molybdenum in direct interaction with the CO molecule. The back-donation into the  $\pi^*$  CO orbital is shown by the two dark rings around the carbon and oxygen atoms. Attempts have also been made to adsorb a CO molecule in a bridging position between two Mo atoms. Whatever the starting configuration, the final geometry always corresponds to the aforementioned top adsorption. Moreover, it appears that only one CO molecule can adsorb per unit cell. Indeed, attempts to adsorb two CO molecules on two vicinal Mo atoms in the cell were performed, but a destabilisation occurs for this configuration since the adsorption energy of the second molecule is negative ( $-0.2$  eV) even if a minimum can be reached. Thus, only one adsorption mode is possible on the [6–3] molybdenum edge for which the stretching wavenumber is calculated at  $2080\text{ cm}^{-1}$ . By comparison with the  $\nu(\text{CO})$  wavenumber of the free molecule, a downward shift of  $60\text{ cm}^{-1}$  is obtained upon adsorption on this edge.

A top adsorption is also possible on the sulphur edge of the [6–3] surface configuration with an adsorption energy of  $0.1$  eV similar to the one obtained with the Mo edge. However, the Mo–C distance is shorter ( $2.06$  versus  $2.08\text{ \AA}$ ) than on the molybdenum edge and the C–O distance longer ( $1.16$  versus  $1.15\text{ \AA}$ ). The  $\nu(\text{CO})$  wavenumber is now calculated at

$2040\text{ cm}^{-1}$ , a value that is in agreement with the C–O distance. The CO molecule is perpendicular to the surface as shown in Fig. 10 that gives the geometry after optimisation. This orientation may allow an important overlap: (i) between the non-bonding CO orbital and the first empty surface state, which is mainly  $\text{d}z^2$  type orbital located on the Mo [14]; (ii) between the empty  $\pi^*$  CO orbital and the last occupied surface states. On the other hand, the distance between the four sulphur atoms and the carbon ( $2.56\text{ \AA}$ ) induces repulsion and lowers the binding energy.

In conditions corresponding to high hydrogen amount, the stable surface configuration is the [3–3] one. The molybdenum edge is the same as on the previous surface and the same CO adsorption mode is therefore obtained. The difference is found on the sulphur edge where three sulphur atoms are removed, creating CUS sites ( $\text{Mo}_{4\text{c}}$  atoms). As a consequence, CO adsorption is much stronger ( $E_{\text{ads}} = 0.7$  eV) and the computed stretching frequency shifts towards lower wavenumbers ( $2000\text{ cm}^{-1}$ ), e.g. a shift of  $80\text{ cm}^{-1}$  by comparison with CO adsorbed on the molybdenum edge. A representation of the optimised structure is given in Fig. 11. An important difference between the molybdenum edge and the reduced sulphur edge is the number of CO molecules that can adsorb per unit cell on the later edge. Indeed as shown in Fig. 11, two CO molecules can adsorb per unit cell on two vicinal Mo atoms (Fig. 11A and B) or on the same one (Fig. 11C). Whatever the adsorption mode, e.g. mono- or dicarbonyl, the adsorption energy per

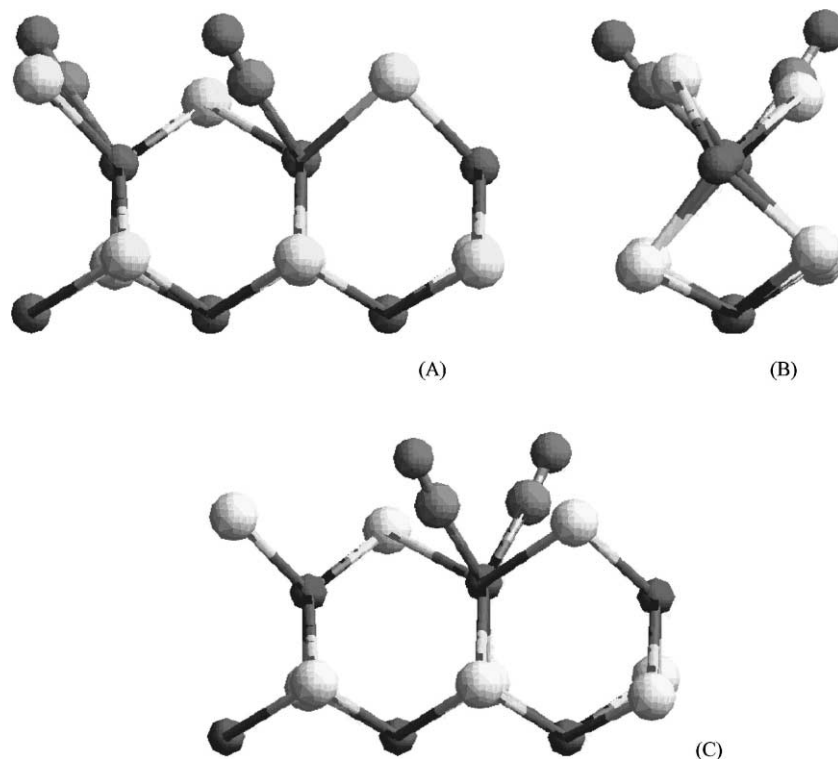


Fig. 11. Optimised configuration for two CO molecules adsorbed on two different molybdenum atoms of the reduced sulphur edge [3-X]: (A) front view; (B) side view; (C) front view of two CO molecules adsorbed on the same molybdenum atom of the reduced sulphur edge [3-X].

CO molecule is the same and corresponds to the value obtained for the adsorption on the Mo edge. The maximum number of CO molecules that can adsorb on this sulphur edge is thus higher than the number that can adsorb on a molybdenum edge and lies between 2-fold and 4-fold the latter one according to the CO uptake. The calculation of the  $\nu(\text{CO})$  stretching wavenumber gives the two  $\nu(\text{CO})$  values at 2035 and 1995  $\text{cm}^{-1}$  for the dicarbonyl geometry (Fig. 11C) and at 2015 and 1965  $\text{cm}^{-1}$  for CO adsorbed on vicinal Mo atoms (Fig. 11A and B). The possibility of various mode of adsorptions on this edge can thus be described as a distribution of sites that should induce a broadening of the IR band.

The last stable surface configuration that we have to consider is the [6–6] one that only exist in H<sub>2</sub>S-rich conditions. Both edge has 6-fold coordinated Mo atoms, but adsorption of CO can only proceed on the sulphur edge as described above for the [6–3] sulphur

edge surface. Indeed, calculations show that CO adsorption on the molybdenum edge is a very endothermic reaction. This is ascribed to the steric hindrance in the direction of the unoccupied orbitals that is much more important and precludes CO adsorption.

#### 4. Discussion

From experimental results, CO adsorption on MoS<sub>2</sub> slabs gives rise at least to four  $\nu(\text{CO})$  bands: (i) a band at 2110–2100  $\text{cm}^{-1}$  which is already observed on the sulphided catalyst; (ii) a weak one at ca. 2130  $\text{cm}^{-1}$  observed at very low CO coverage or in the case of a partial poisoning of the Mo sites by H<sub>2</sub>S; (iii) a band at 2100–2095  $\text{cm}^{-1}$  which appears after reduction of the sulphided phase; (iv) a broad feature at 2075–2020  $\text{cm}^{-1}$  which is already present after sulphidation and develops under reductive treatment. The

question, which evidently arises, is to which specific sites of the MoS<sub>2</sub> slabs correspond these  $\nu(\text{CO})$  bands.

The downwards shift of the  $\nu(\text{CO})$  wavenumber as compared with the gas phase, observed upon adsorption on MoS<sub>2</sub>-based catalysts, has deal to lot of discussions about the oxidation degree of the Mo sites. It is generally proposed that the shift of the CO stretching mode is due to a lower oxidation degree of the Mo atom that would present an oxidation degree of +2 or even lower [4–6,11,12]. However, direct evidences of these lower oxidation degrees have never been given by XPS. This discrepancy could be related to the fact that XPS characterised both bulk and surface Mo, whereas CO adsorption specifically probes surface Mo atoms. Molybdenum is a very versatile element, which can adopt many oxidation states and coordination. Even if the question of the oxidation degree of the Mo edges still exists, another way to interpret the shift is to consider the probe molecule as a ligand that interacts with Mo atoms of the edge, the coordination of which depends on the surrounding atmosphere.

Taking into account the crystallographic structure of the MoS<sub>2</sub> crystallites, two types of edge were considered, i.e. the sulphur edge and the molybdenum edge. CO adsorption may proceed on both the edges. The appearance of mainly one symmetrical  $\nu(\text{CO})$  band (2110 cm<sup>-1</sup>) with a tail at lower wavenumbers (ca. 2075 cm<sup>-1</sup>) on the sulphided molybdenum catalysts allows one to deduce that CO is essentially adsorbed on two kinds of Mo site after such a treatment. Calculation shows that, in sulphiding conditions, the stable configuration exhibits [6–3] surface according to our nomenclature. In this configuration, the Mo sites of the molybdenum edges, which are Mo<sub>6c</sub> ones, can adsorb CO as schematically represented in Fig. 9A. Calculations show that this adsorption configuration induces a shift towards low wavenumber of 60 cm<sup>-1</sup> compared to the frequency of the free CO molecule. The band observed at 2110 cm<sup>-1</sup> can be assigned to the  $\nu(\text{CO})$  vibration of molecules adsorbed on these molybdenum sites (Mo<sub>6c</sub>) of the molybdenum edges, since it presents a downwards shift of 30 cm<sup>-1</sup>, which is in rather good agreement with calculations. This attribution is also in accordance with the low value of the calculated adsorption energy as this band disappears by outgassing the catalyst at RT.

On the other hand, the tail observed at low wavenumbers (ca. 2075 cm<sup>-1</sup>) could be due to CO

adsorbed on the sulphur edge of the [6–3] surface since in this case, the calculated  $\nu(\text{CO})$  shift is 40 cm<sup>-1</sup> with respect to CO adsorption on the Mo edge, which nicely corresponds to the experimental shift. However, it should be noted that the thermal stability of this species is higher than that giving rise to the band at 2110 cm<sup>-1</sup>, although calculations indicate the same adsorption energy for both sites (see Table 1).

Qualitative agreement between experiments and calculation are also obtained upon increasing the sulphur coverage of the MoS<sub>2</sub> slabs. Indeed, H<sub>2</sub>S introduction on the sulphided catalyst, progressively hinder CO adsorption in agreement with our DFT calculations that show that in rich sulphur atmosphere, both molybdenum and sulphur edge sites are saturated. Calculation showed that adsorption on the molybdenum edge (Mo<sub>6c</sub>) is not possible, whereas adsorption on the sulphur edge may occur as discussed above.

If a reductive treatment is performed on the sulphided catalyst, modifications of the spectra of adsorbed CO are evidenced that should be assigned to the creation of new Mo sites. An augmentation and a broadening of the low wavenumber features around 2075–2050 cm<sup>-1</sup> occur as already reported, and a band at 2100–2095 cm<sup>-1</sup>, never quoted in the literature, appears. It should be mentioned that previous studies do not report metallic Mo to be formed after such reductive treatments [4]. Calculation indicates that upon reduction, the surface transforms into a [3–3] one, where the molybdenum edge remains unchanged in agreement with the persistence of the band at 2110 cm<sup>-1</sup>. On the sulphur edge, Mo<sub>4c</sub> are formed on which CO adsorption may also proceed. An increase in the CO uptake after reduction is therefore expected. From our DFT calculations, the band characteristic of CO adsorbed on these Mo sites should be observed at lower wavenumber than for CO adsorption on molybdenum edge. A wavenumber decrease of at least 115 cm<sup>-1</sup> depending on the adsorption configuration is calculated. Taking into account calculated CO wavenumber shift, the bands at 2055–2020 cm<sup>-1</sup> could be assigned to CO adsorption on the reduced sulphur edges. Moreover, the absence of intensity variation of this band upon degassing at 100 K (Fig. 6) is in agreement with the high adsorption energy (0.7 eV) of CO on these sites. Calculations indicate that various configurations of adsorption are possible on this kind of edges, e.g. monocarbonyl on vicinal Mo atoms and/or

dicarbonyl adsorption configuration. This could explain the broadness of the low wavenumber features.

In a previous study [6], the low wavenumber band which develops after reduction of the catalyst was attributed to CO adsorption on corner sites. Indeed, the authors envisage that corner sites present a lower sulphur coordination number than edge ones. However, our calculations show that the coordination number of surface sites is difficult to presume because strong reorganisation of the surface occurs when sulphur atoms are eliminated. Therefore, modelisation of corner sites should be done to confirm or infer such attribution. At this stage of our investigation, we consider that this low wavenumber  $\nu(\text{CO})$  corresponds to CO in interaction with Mo atoms of lower coordination, mainly arising upon reduction.

Experiments performed on an ex situ sulphided catalyst show that an irreversible poisoning of the Mo sites occurred. It is interesting to note that the sensitivity of the  $2110\text{ cm}^{-1}$  band to air contact is higher than the  $2050\text{--}2075\text{ cm}^{-1}$  one. From the previous attribution, one can consider that the metallic edge sites of the [6–3] surface are more easily poisoned by laboratory atmosphere than the sulphur edge.

Some sites remain however unidentified. Indeed the high wavenumber band at  $2130\text{ cm}^{-1}$ , which is observed when few amounts of CO are adsorbed on the sulphided catalyst, is not attributed. Moreover, the reduction also leads to the appearance of a band at  $2095\text{ cm}^{-1}$ . Its wavenumber very close to that of CO adsorbed on the  $\text{Mo}_{6c}$  sites of metallic edges ( $2110\text{ cm}^{-1}$ ) discards its attribution to adsorption on reduced sulphur edge sites ( $\text{Mo}_{4c}$ ). An intermediate coordination of Mo ( $\text{Mo}_{5c}$ ) has to be considered and calculations are in progress to interpret this band.

## 5. Conclusion

This paper reported an investigation of carbon monoxide adsorption on sulphided Mo catalysts by means of IR spectroscopy and ab initio calculations. Both techniques show that the surface state of the sulphided phase is strongly modified by post-treatment with  $\text{H}_2$  or  $\text{H}_2\text{S}$ . The parallel between experimental and calculated results on  $\text{MoS}_2$  allowed us to attribute the main  $\nu(\text{CO})$  bands. Results may be summarised as follows:

- After sulphidation,  $\nu(\text{CO})$  spectra mainly consist in: (i) an intense band at ca.  $2110\text{ cm}^{-1}$ ; (ii) a tail at lower wavenumbers. These bands are, respectively, attributed to CO adsorption on: (i) 6-fold coordinated Mo of the molybdenum edge and (ii) 6-fold coordinated Mo of the sulphur edge of  $\text{MoS}_2$  crystallites exhibiting [6–3] surfaces.
- After a reductive treatment, new features appear: (i) below  $2080\text{ cm}^{-1}$ , the tail of  $\nu(\text{CO})$  band develops and spreads down to  $2000\text{--}2020\text{ cm}^{-1}$ ; (ii) a band at  $2095\text{ cm}^{-1}$  develops. These features are attributed to CO adsorption on: (i) 4-fold coordinated Mo of the reduced sulphur edge under the form of mono- or dicarbonyl species; (ii) possibly 5-fold coordinated Mo atoms.
- A weak, hardly visible band at ca.  $2130\text{ cm}^{-1}$  could not be attributed with our model.

Finally, this first confrontation of results issued from experiments and theoretical calculations allows a better understanding of the surface-site configuration, by the way it confirms that the calculated surfaces are suitable for surface modelisation.

## Acknowledgements

This work has been performed within the GDR “Dynamique moléculaire quantique appliquée à la catalyse et à l’adsorption” supported by IFP, Total-Fina, CNRS and TU Wien. The authors wish to thank J.S. Filhol for help in the frequency calculations. SC wishes to thank TOTALFINAELF for financial support.

## References

- [1] Z. Shuxian, W.K. Hall, G. Ertl, H. Knözinger, J. Catal. 100 (1986) 167.
- [2] L. Portela, P. Grange, B. Delmon, Catal. Rev.: Sci. Eng. 37 (1995) 699.
- [3] J. Bachelier, J.-C. Duchet, D. Cornet, Bull. Soc. Chim. Belg. 90 (1981) 1301.
- [4] J.B. Peri, J. Phys. Chem. 86 (1982) 1615.
- [5] J. Bachelier, M.J. Tilliette, M. Cornac, J.-C. Duchet, J.-C. Lavalley, D. Cornet, Bull. Soc. Chim. Belg. 93 (1984) 743.
- [6] B. Müller, A.D. van Langeveld, J.A. Moulijn, H. Knözinger, J. Phys. Chem. 97 (1993) 9028.
- [7] X. Qin, G. Xiexian, R. Prada Silvy, P. Grange, B. Delmon, in: Proceedings of the Ninth International Congress on Catalysis, Vol. 1, Calgary, Canada, 1988, p. 66.

- [8] F. Maugé, J.-C. Lavalley, *J. Catal.* 69 (1992) 137.
- [9] P. Da Silva, Ph.D. Thesis, University of Paris VI, France, 1998.
- [10] A. Travert, Ph.D. Thesis, University of Caen, France, 2000.
- [11] M.I. Zaki, B. Vielhaber, H. Knözinger, *J. Phys. Chem.* 90 (1986) 3176.
- [12] E. Delgado, G.A. Fuentes, G. Hermann, G. Kunzmann, H. Knözinger, *Bull. Soc. Chim. Belg.* 93 (1984) 743.
- [13] P. Raybaud, J. Hafner, G. Kresse, H. Toulhoat, *Surf. Sci.* 407 (1998) 237.
- [14] P. Raybaud, Ph.D. Thesis, Université Paris VI, France, 1998.
- [15] P. Raybaud, J. Hafner, G. Kresse, S. Kasztelan, H. Toulhoat, *J. Catal.* 189 (2000) 129.
- [16] S. Cristol, J.F. Paul, E. Payen, D. Bougeard, F. Hutschka, *J. Phys. Chem.* 104 (2000) 11290.
- [17] G. Kresse, J. Hafner, *Phys. Rev. B* 47 (1993) 558.
- [18] G. Kresse, J. Hafner, *Phys. Rev. B* 49 (1994) 14521.
- [19] G. Kresse, J. Furthmüller, *Comput. Mater. Sci.* 6 (1995) 15.
- [20] G. Kresse, J. Furthmüller, *Phys. Rev. B* 54 (1996) 11169.
- [21] M. Methfessel, A.T. Paxton, *Phys. Rev. B* 40 (1989) 3616.
- [22] J.P. Perdew, A. Zunger, *Phys. Rev. B* 23 (1981) 5048.
- [23] J.P. Perdew, J.A. Chevary, S.H. Vosko, K.A. Jackson, M.R. Pedersen, D.J. Singh, C. Frolais, *Phys. Rev. B* 46 (1992) 6671.
- [24] F.E. Massoth, C.S. Kim, J.W. Cui, *Appl. Catal.* 58 (1990) 58.